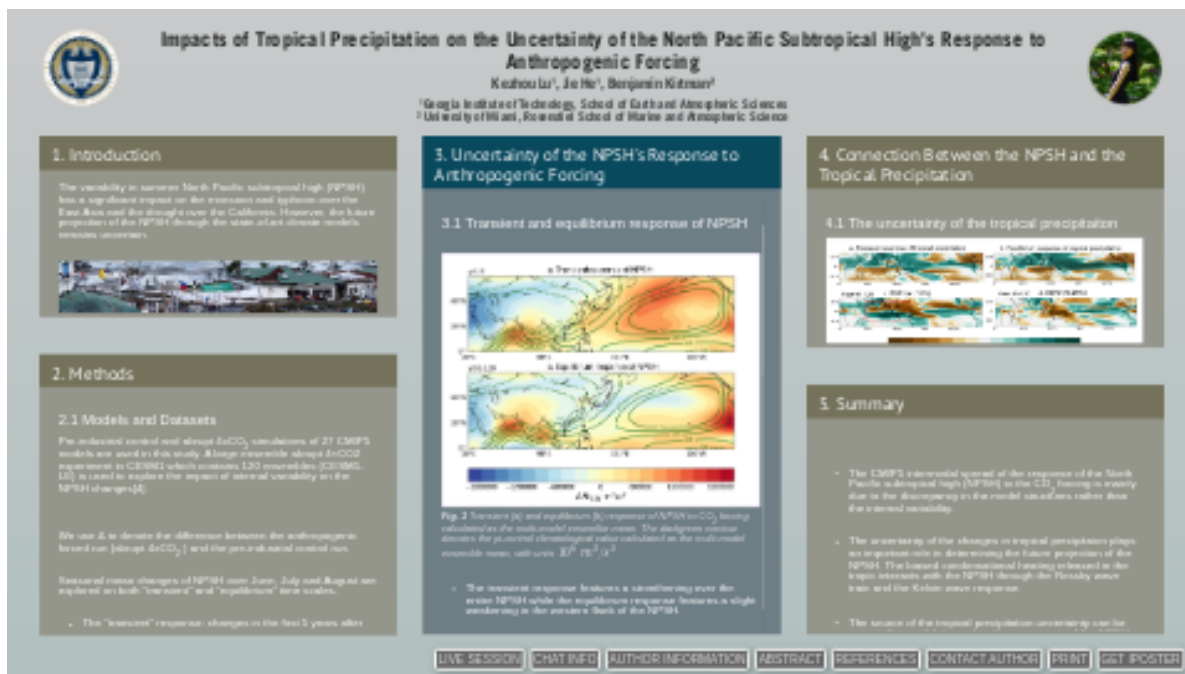


# Impacts of Tropical Precipitation on the Uncertainty of the North Pacific Subtropical High's Response to Anthropogenic Forcing



Kezhou Lu<sup>1</sup>, Jie He<sup>1</sup>, Benjamin Kirtman<sup>2</sup>

<sup>1</sup>Georgia Institute of Technology, School of Earth and Atmospheric Sciences

<sup>2</sup> University of Miami, Rosenstiel School of Marine and Atmospheric Science



PRESENTED AT:

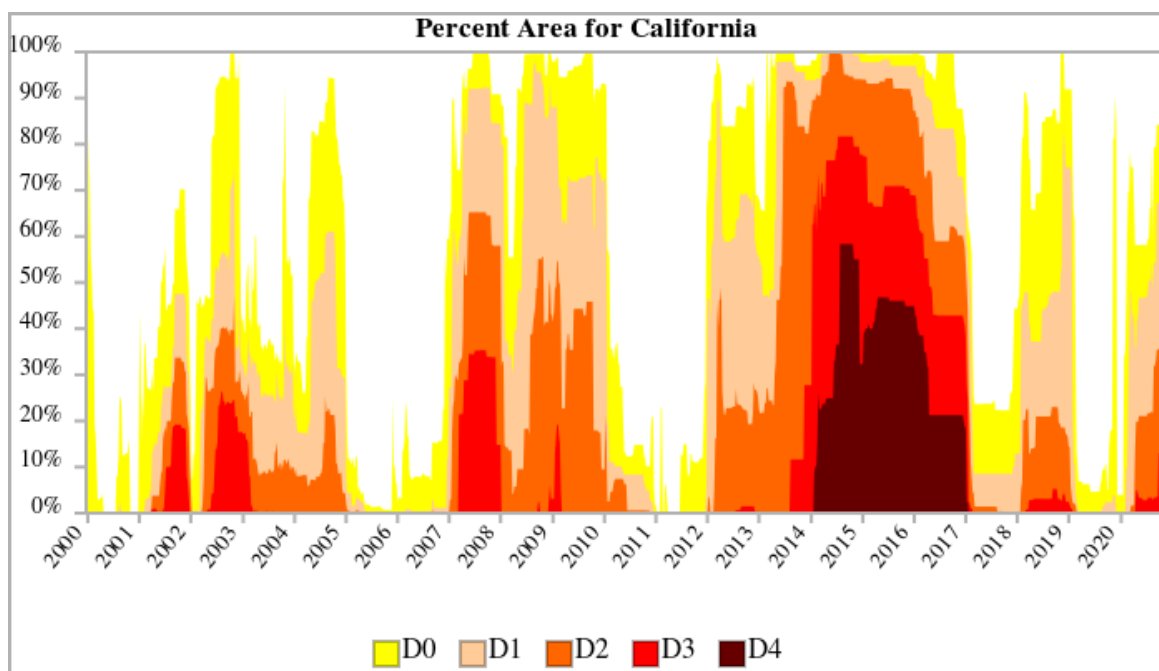


# 1. INTRODUCTION

The variability in summer North Pacific subtropical high (NPSH) has a significant impact on the monsoon and typhoon over the East Asia and the drought over the California. However, the future projection of the NPSH through the state-of-art climate models remains uncertain.



*Discontruction in Tacloban, Philippines from Typhoon Haiyan in 2013*



*Drought in California from 2000 to 2020 (<https://www.drought.gov/drought/states/california>)*

Several mechanisms have been proposed to explain the uncertainty of the NPSH projection, including the radiative forcing and the subsequent surface changes associated with land-sea thermal contrast, mean sea surface temperature (SST) warmings, the bias of tropical SST pattern and the bias in the marine stratocumulus [1-3]. However, the uncertainty contributed by the tropical precipitation hasn't been largely explored.

In this research, we explore the connection between tropical precipitation uncertainty and the NPSH uncertainty through both fully coupled global circulation models and a simple atmospheric primitive equation model.

## 2. METHODS

### 2.1 Models and Datasets

Pre-industrial control and abrupt 4xCO<sub>2</sub> simulations of 27 CMIP5 models (<https://esgf-node.llnl.gov/projects/cmip5/>) are used in this study. A large ensemble abrupt 4xCO<sub>2</sub> experiment in CESM1 which contains 120 ensembles (CESM1-LE) is used to explore the impact of internal variability on the NPSH changes[4].

We use  $\Delta$  to denote the difference between the anthropogenic forced run (abrupt 4xCO<sub>2</sub>) and the pre-industrial control run.

Seasonal mean changes of NPSH over June, July and August are explored on both "transient" and "equilibrium" time scales.

- The "transient" response: changes in the first 5 years after CO<sub>2</sub> quadrupling.
- The "equilibrium" response: changes averaged over year 91 to year 120 in the abrupt 4xCO<sub>2</sub> simulations.

As the subtropical circulation changes can be affected by both the direct CO<sub>2</sub> forcing and subsequent surface temperature changes, and the global mean sea surface temperature (SST) warming, we choose abrupt 4xCO<sub>2</sub> to dissect different mechanisms based on their distinct time scales [1, 4].

In addition, an ideal dry-core model with spectral in the horizontal and finite sigma level on the vertical is used to explore the connection between tropical diabatic heating and circulation changes. The dry-core model has the horizontal resolution of 128 longitudes and 106 Gaussian latitudes, and 26 vertical levels. All the moist related processes are excluded. Newtonian relaxation towards the pre-industrial climate state is applied with a timescale of 10 days over the top 10 layers, 5 days within the bottom 3 layers and 25 days over the rest of the atmosphere. The diabatic heating is prescribed at each time step following the thermodynamic equation:

$$\frac{\partial T}{\partial t} = \frac{\dot{Q}}{c_p} - \vec{v} \cdot \nabla T + \omega \left( \frac{RT}{p c_p} - \frac{\partial T}{\partial p} \right)$$

### 2.2 Quantify the internal variability

The standard deviation of the zonally asymmetric component of 925hpa stream function ( $\Delta \Psi_{925}$ ) pattern among 120 ensembles from CESM1-LE is quantified as the changes due to internal variability.

### 2.3 Quantify the intermodel spread

The leading modes of intermodel uncertainty in the NPSH responses in the domain (10–50°N, 110–240°E) is analyzed via the typical EOF analysis but applied to model-spatial dimension:

$$\Delta\psi_{s2f}^*(m,s) = \sum_{i=1}^n PC_{m,i} \cdot EOF_{i,s}$$

where \* denotes the deviation from the multi-model ensemble mean, m is the number of models, s is the number of grid points and i represents the ith modes of the EOF.

### 3. UNCERTAINTY OF THE NPSH'S RESPONSE TO ANTHROPOGENIC FORCING

#### 3.1 Transient and equilibrium response of NPSH

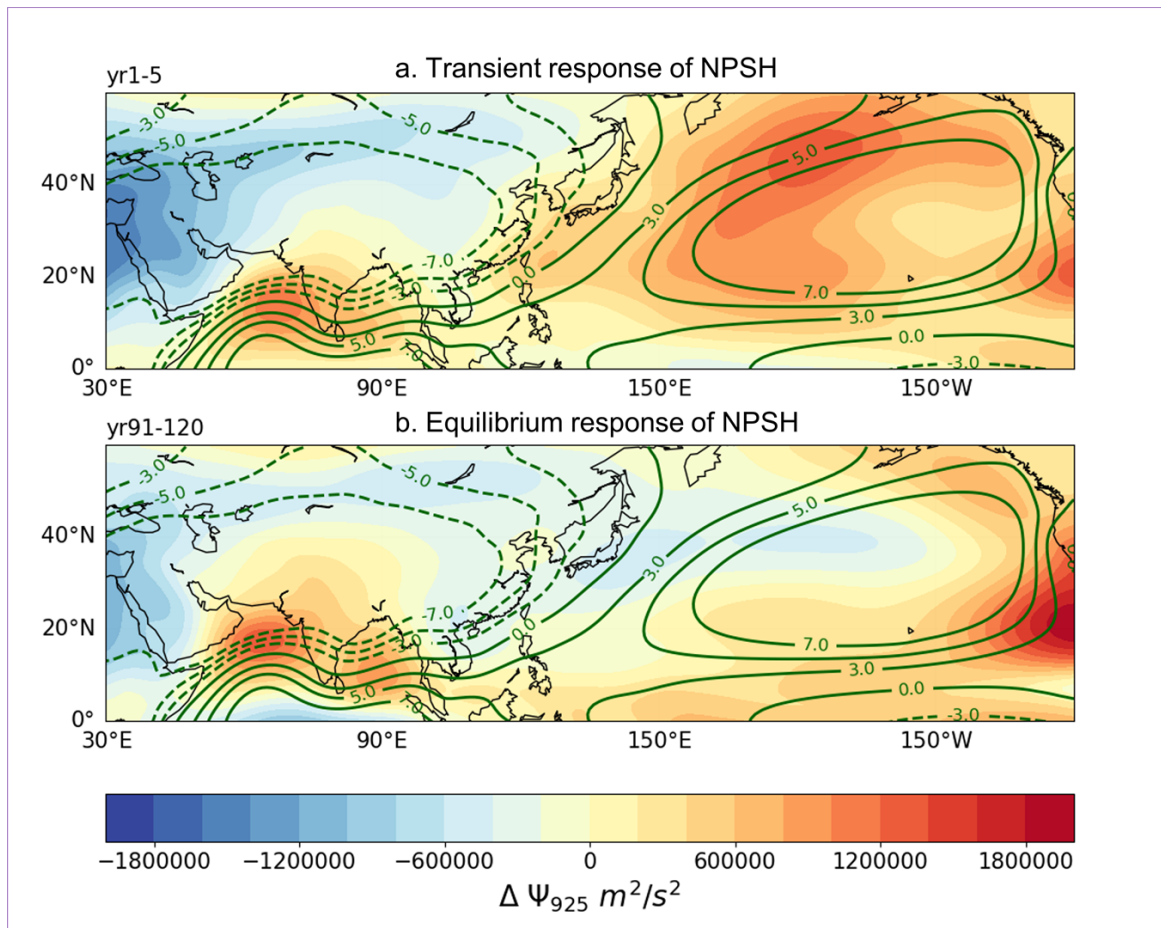


**Fig. 1** Transient (a) and equilibrium (b) response of NPSH to CO<sub>2</sub> forcing calculated as the multi-model ensemble mean. The darkgreen contour denotes the pi-control climatological value calculated as the multi-model ensemble mean, with units  $10^6 m^2/s^2$

- The transient response features a strengthening over the entire NPSH while the equilibrium response features a slight weakening in the western flank of the NPSH.

#### 3.2 Leading modes of uncertainty



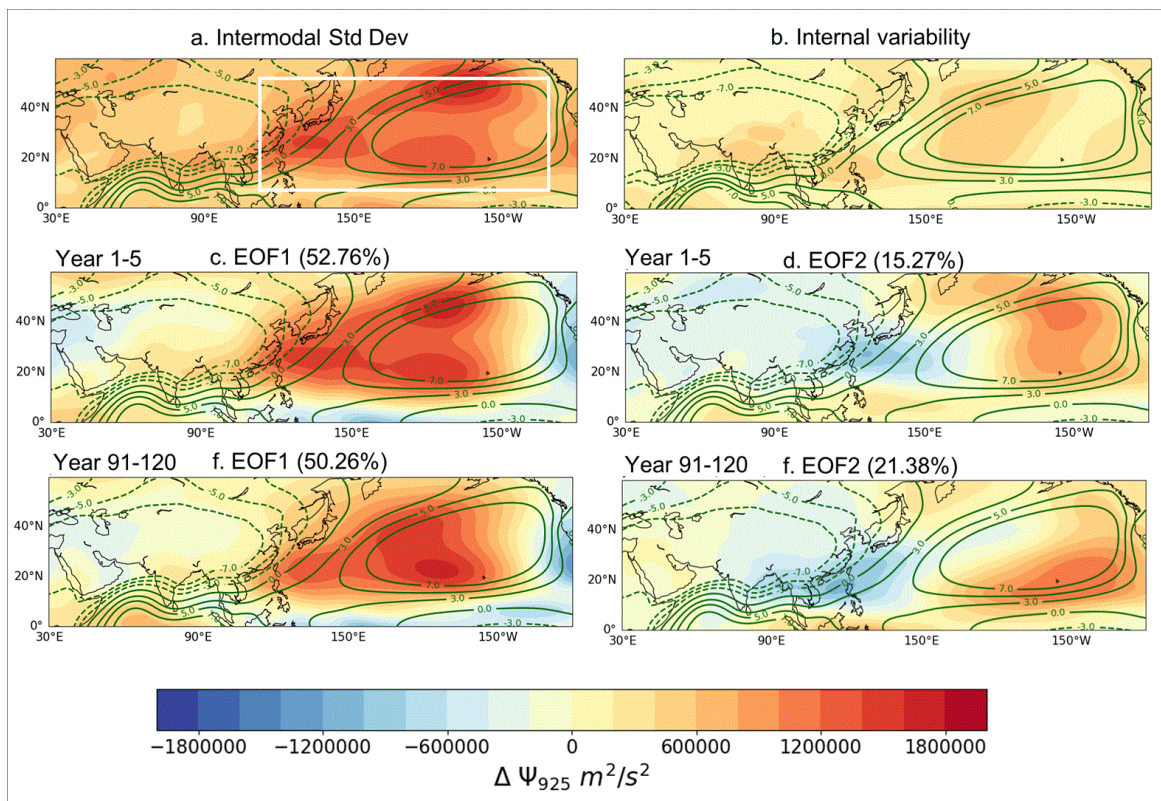


**Fig. 2** Uncertainty of the response of NPSH to anthropogenic forcing. (a) The total intermodal spread calculated as intermodal standard deviation. (b) Uncertainty due to internal variability calculated as the standard deviation among all the ensembles in CESM1-LE. (b-f) The two leading modes (EOF1 and EOF2) derived from intermodal EOF analysis on both transient (year 1-5) and equilibrium time scales. The EOF modes are represented by regressing  $\Delta\Psi_{925}$  onto the corresponding first and second normalized principle components (PC1 and PC2). The white box in (a) denotes the region (10–50°N, 110–240°E) where EOF analysis is performed. The darkgreen contour is the climatological pre-industrial value same as Fig. 1. Value in the parentheses is intermodel variance explained by corresponding mode.

- The intermodal spread is mostly contributed by the different model structures rather than the internal variability (compare Figs. 2a and 2b).
- The intermodal spread is well captured by the first mode on both time scales (compare Figs. 2a, 2c and 2f). The first mode features an overall strengthening of the NPSH, while the second mode features a weakening (strengthening) in the western (eastern) parts of the NPSH during transient time period, and a weakening (strengthening) in the northwestern (southeastern) parts of the NPSH during the equilibrium time period.
- The leading mode of uncertainty is qualitatively similar for both transient and equilibrium response, suggesting the transient response uncertainty accounts for a substantial portion (more than 50%) of the total uncertainty.

## 4. CONNECTION BETWEEN THE NPSH AND THE TROPICAL PRECIPITATION

### 4.1 The uncertainty of the tropical precipitaiton

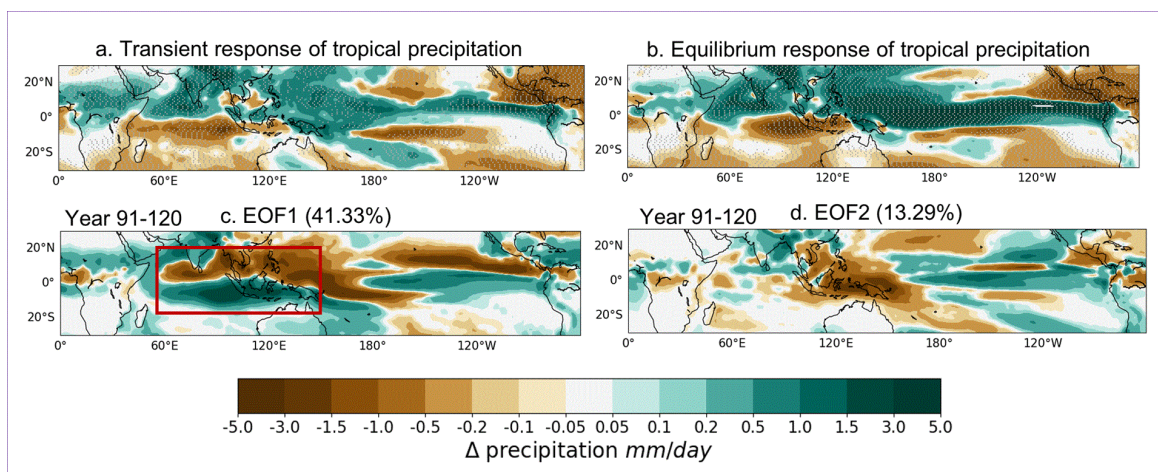


**Fig. 3** The transient (a) and equilibrium (b) tropical precipitation response calculated as the multi-model ensemble mean. The model spread patterns of precipitation changes, shown in (c) and (d), are calculated by performing similar EOF analysis as  $\Delta \Psi_{925}$  but on Indo-West Pacific (20°S–20°N, 60–150°E, red box in (c)) precipitation changes. The stipplings in (a) and (b) are areas where more than 70% models agree with the sign change.

- On both time scales, enhanced precipitations are found over Africa, South East Asia, Maritime continent, and equatorial Pacific. Meanwhile, there is also a dipole pattern features more (less) precipitation over Northern (Southern) Indian Basin. The overall tropical response patterns agree with the "wet-get-wetter" paradigm [5, 6].
- The first leading mode of tropical precipitation uncertainty features an opposite dipole structure over Indo-West Pacific region (compare Figs. 3a, 3b and 3c) and accounts for 41.33% of the total uncertainty. The second leading mode features an overall drying over the Maritime Continents. Both EOF1 and EOF2 have an enhanced precipitation over Central and Eastern equatorial Pacific.

### 4.2 Connection between tropical precipitation uncertainty and the NPSH uncertainty



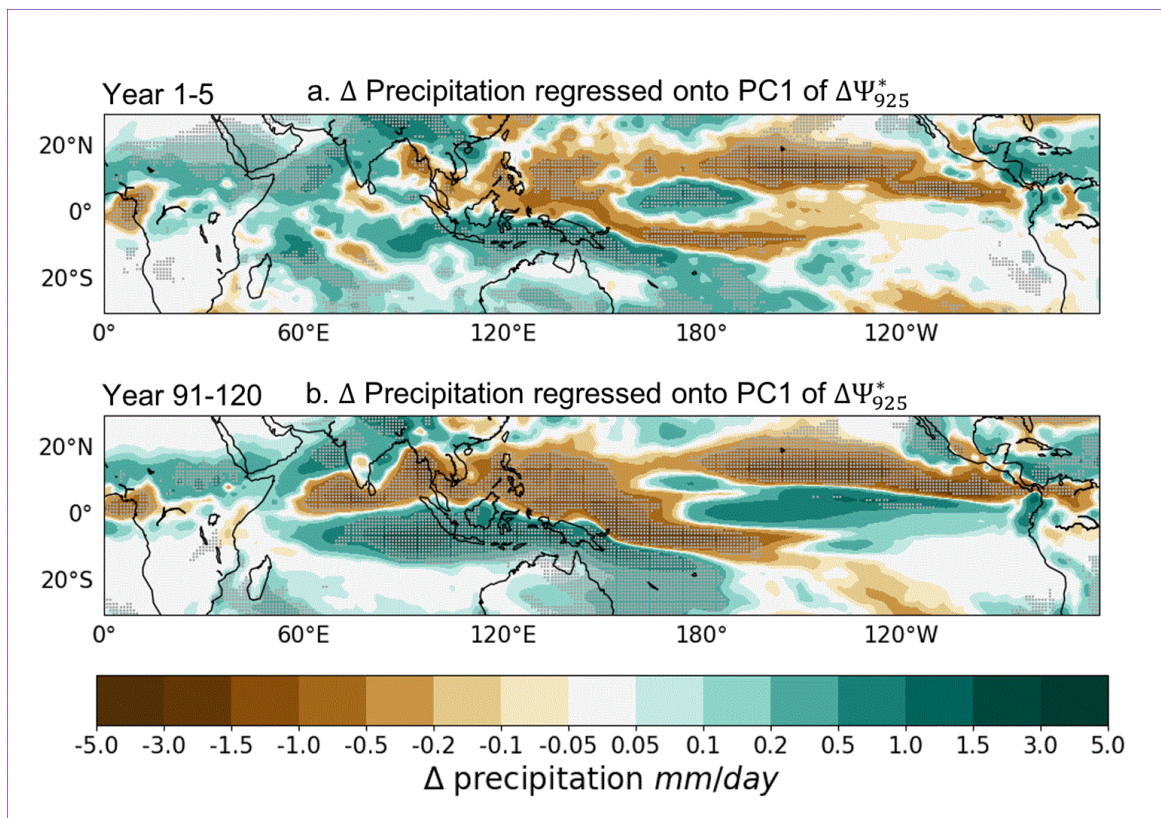


**Fig. 4** The model spread patterns of precipitation changes in both transient (a) and equilibrium (b) associated with PC1 of  $\Delta\Psi_{925}^*$ . Stipplings regions are statically significant at the 5% level based on Student t-test.

- The intermodal spread patterns of precipitation changes associated with the uncertainty of the NPSH are viturally similar on both transient and equilibrium times scles, with a "monsoon-like" precipitation enhancement over Africa, East Asia and Australia (Figs. 4a and 4b)
- The uncertainty of tropical precipitation changes regressed onto PC1 of the NPSH (Figs. 4a and 4b) are very similar to the leading mode of the tropical precipitation uncertainty (Fig. 3c). This similarity suggests that source of the tropical precipitation uncertainty can potentially be important to explain the uncertainty of the NPSH.
- The impact of the tropical precipitation uncertainty on the NPSH is further explored though the idealized dry-core model. The intermodal spread pattern in Fig. 3c is converted to the condensational heating (or cooling) pattern and then prescribed as a constant diabatic forcing into the dry-core model. The resultant response of the NPSH is shown below:

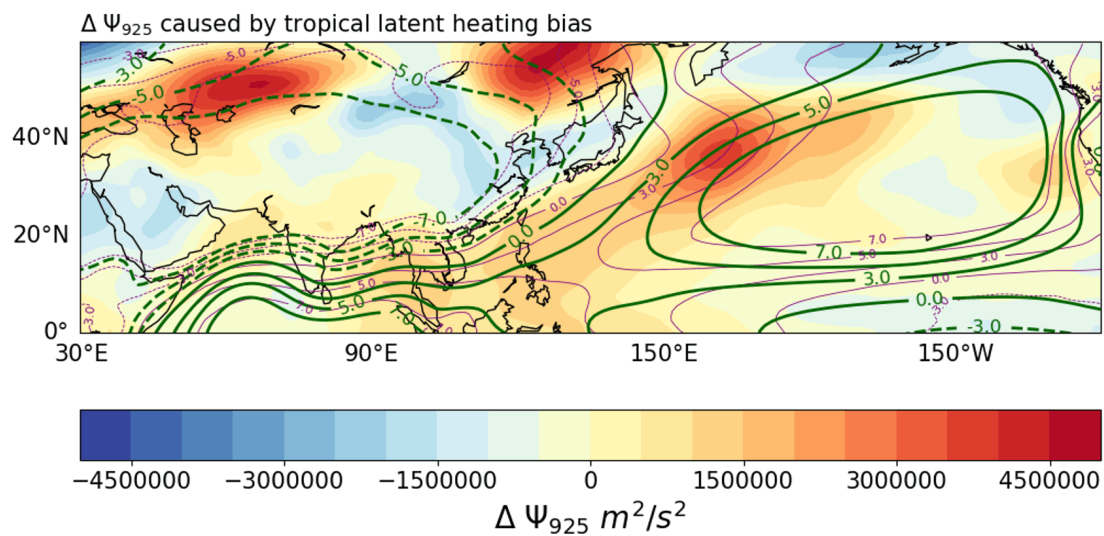


**Fig. 5** The changes in the NPSH caused by the intermodal spread of the tropical precipitation. The thick darkgreen contour is the pre-industrial control climatology from CMIP5 multi-model ensemble mean (same as Fig.1 and Fig.2). The thin purple contour is the control climatology of the idealized dry-core model (i.e. without additional diabatic forcing).

- The tropical precipitation uncertainty induces a strengthening over the western part of the NPSH and a weakening over the northeastern part.
- The strengthening can be viewed as the Kelvin wave response to the "monsoon-like" heating over the East Asia [7].
- The tropical diabatic uncertainty can also interact with the NPSH through the Rossby wave trains [7, 8].

## 5. SUMMARY

- The CMIP5 intermodal spread of the response of the North Pacific subtropical high (NPSH) to the CO<sub>2</sub> forcing is mainly due to the discrepancy in the model structures rather than the internal variability.
- The uncertainty of the changes in tropical precipitation plays an important role in determining the future projection of the NPSH. The biased condensational heating released in the tropic interacts with the NPSH through the Rossby wave train and the Kelvin wave response.
- The source of the tropical precipitation uncertainty can be potentially possible to explain the uncertainty of the NPSH under the anthropogenic forced climate change.

## AUTHOR INFORMATION

### About me

I am a third-year PhD student from Georgia Institute of Technology. My advisor is [Jie He](https://he.eas.gatech.edu/index.html) (<https://he.eas.gatech.edu/index.html>).

My research interests are:

- The anthropogenic forced responses of tropical hydroclimate and atmospheric circulation.
- Connection between tropical and subtropical precipitation changes
- Uncertainties in climate projections of subtropical cyclones.

Please contact me if you have any questions: [kezhou.lu@eas.gatech.edu](mailto:kezhou.lu@eas.gatech.edu)

## ABSTRACT

The variability in summer North Pacific subtropical high (NPSH) has a significant impact on the monsoon and typhoon over the East Asia and the drought over the California. However, the future projection of the NPSH through the state-of-art climate models, particularly those pertaining to the tropical precipitation uncertainty remain unclear. In this research, we explore the connection between tropical precipitation uncertainty and the NPSH uncertainty through both fully coupled global circulation models from CMIP5 and a dry-core atmospheric primitive equation model. We have found that the biased condensational heating released through the tropic precipitation interacts with the NPSH through the Rossby wave train and the Kelvin wave response. The source of the tropical precipitation uncertainty can be potentially responsible for the uncertainty of the NPSH under the anthropogenic forced climate change.



## REFERENCES

- [1] Shaw, T. A., & Voigt, A. (2015). Tug of war on summertime circulation between radiative forcing and sea surface warming. *Nature Geoscience*, 8 (7), 560–566. Retrieved from <https://doi.org/10.1038/ngeo2449> doi: 10.1038/ngeo2449
- [2] Chen, X., Zhou, T., Wu, P. et al. Emergent constraints on future projections of the western North Pacific Subtropical High. *Nat Commun* 11, 2802 (2020). <https://doi.org/10.1038/s41467-020-16631-9>
- [3] Zhou, Z., & Xie, S. (2015). Effects of Climatological Model Biases on the Projection of Tropical Climate Change, *Journal of Climate*, 28(24), 9909-9917. Retrieved Dec 15, 2020, from <https://journals.ametsoc.org/view/journals/clim/28/24/jcli-d-15-0243.1.xml>
- [4] Lu, K., He, J., Boniface, F., & Rugenstein, M. A. A. (2020). Mechanisms of Fast Walker Circulation Responses to CO2 Forcing. Retrieved from

### **Mechanisms of Fast Walker Circulation Responses to CO2 Forcing**

- [5] Xie, S.-P., , C. Deser, , G. A. Vecchi, , J. Ma, , H. Teng, , and A. T. Wittenberg, 2010: Global warming pattern formation: Sea surface temperature and rainfall. *J. Climate*, 23, 966–986, doi:10.1175/2009JCLI3329.1.
- [6] Held, I. M., , and B. J. Soden, 2006: Robust responses of the hydrological cycle to global warming. *J. Climate*, 19, 5686–5699, doi:10.1175/JCLI3990.1.
- [7] Rodwell, M. J., & Hoskins, B. J. (2001). Subtropical Anticyclones and Summer Monsoons, *Journal of Climate*, 14(15), 3192-3211. Retrieved Dec 15, 2020, from [https://journals.ametsoc.org/view/journals/clim/14/15/1520-0442\\_2001\\_014\\_3192\\_saasm\\_2.0.co\\_2.xml](https://journals.ametsoc.org/view/journals/clim/14/15/1520-0442_2001_014_3192_saasm_2.0.co_2.xml)
- [8] Webster, P. J., and J. R. Holton, 1982: Cross-equatorial response to middle-latitude forcing with a latitudinally and zonally nonuniform basic state. *J. Atmos. Sci.*, 39, 722–733